Regenerative Therapy 22 (2023) 128–135

Contents lists available at ScienceDirect

Regenerative Therapy

journal homepage: http://www.elsevier.com/locate/reth

Original Article

Preclinical evaluation of the effect of periodontal regeneration by carbonate apatite in a canine one-wall intrabony defect model

Shunsuke Takeuchi [a], Shunsuke Fukuba [a, *], Munehiro Okada [a], Kohei Nohara [a], Ryo Sato [a], Daichi Yamaki [a], Takanori Matsuura [a], Shu Hoshi [a], Kazuhiro Aoki [b], Takanori Iwata [a]

[a] Department of Periodontology, Graduate School of Medical and Dental Sciences, Tokyo Medical and Dental University, Tokyo, Japan
[b] Department of Basic Oral Health Engineering, Graduate School of Medical and Dental Sciences, Tokyo Medical and Dental University, Tokyo, Japan

ARTICLE INFO

Article history:
Received 16 December 2022
Received in revised form
4 January 2023
Accepted 9 January 2023

Keywords:
Periodontitis
Beagle dogs
Carbonate apatite
Intrabony defects
Periodontal regeneration

ABSTRACT

Objective: This study aimed to histologically compare periodontal regeneration of one-wall intrabony defects treated with open flap debridement, β-tricalcium phosphate (β-TCP), and carbonate apatite (CO_3Ap) in dogs.
Methods: The mandibular third premolars of four beagle dogs were extracted. Twelve weeks after the extraction, a one-wall bone defect of 4 mm × 5 mm (mesio-distal width × depth) was created on the distal side of the mandibular second premolar and mesial side of the fourth premolar. Each defect was randomly allocated to open flap debridement (control group), periodontal regeneration utilizing β-TCP, or CO_3Ap. Eight weeks after the surgery, histologic and histometric analyses were performed.
Results: No ankylosis, infection, or acute inflammation was observed at any of the experimental sites. Newly formed bone and cementum were observed in all experimental groups. The mineral apposition rate of the alveolar bone crest was higher in the CO_3Ap group than in the control and β-TCP groups. The ratio of the new bone area was significantly higher in the CO_3Ap group than in the control group ($P < 0.05$). The bone contact percentage of the residual granules was significantly higher in the CO_3Ap group than in the β-TCP group ($P < 0.05$).
Conclusion: Although this study has limitations, the findings revealed the safety and efficacy of CO_3Ap for periodontal regeneration in one-wall intrabony defects in dogs, and CO_3Ap has a better ability to integrate with bone than β-TCP.

1. Introduction

Periodontitis is an inflammatory disease caused by microorganisms. As gingival inflammation develops around the teeth, attachment loss and bone resorption increase, eventually leading to tooth loss. Intrabony defects under insufficient periodontal treatment have been reported as a high-risk indicator of tooth loss [1]. Thus, appropriate periodontal treatment and management of intrabony defects are important for long term survival of teeth. Periodontal regeneration therapy has been developed for this purpose. This procedure is based on the use of biomaterials such as barrier membranes, bone grafting materials that can support soft tissue and stabilize blood clots, or a combination of both approaches. In general, maintaining space for periodontal tissue regeneration and blood clot stability is easy to achieve in contained defects, such as three-wall intrabony defects. On the other hand, the use of biomaterials is recommended for non-contained defects, such as one- or two-wall intrabony, to maintain the regenerative space and prevent epithelial migration [2].

Autogenous bone grafts, the gold standard for bone grafting, exhibit osteogenesis, osteoinductivity, and osteoconductivity. However, autograft harvesting results in limited volume and requires other surgical sites. Furthermore, resorption rate of autogenous bone grafts is fast in general and the volume of periodontal tissue regeneration is unpredictable [3]. From this point of view, using alternative bone graft materials like allogeneic, alloplastic and xenogetic bone

Abbreviations: HA, Hydroxyapatite; β-TCP, β-tricalcium phosphate; CO_3Ap, Carbonate apatite; MAR, Mineral apposition rate; ABH, Alveolar bone height; NBA, New bone area; DBBM, Deproteinized bovine bone mineral.

* Corresponding author. Department of Periodontology, Graduate School of Medical and Dental Science, Tokyo Medical and Dental University, 1-5-45 Yushima, Bunkyo-ku, Tokyo, 113-8510, Japan. Fax: +81 3 5803 0196.
E-mail address: sfukuba.peri@tmd.ac.jp (S. Fukuba).

Peer review under responsibility of the Japanese Society for Regenerative Medicine.

https://doi.org/10.1016/j.reth.2023.01.002

grafts avoid the need to create a donor site. However, infections, immunogenic rejection, and the risk of disease transmission remain problems with allogeneic and xenogetic bone grafts [4]. To overcome these problems, various alloplastic bone graft materials, particularly calcium phosphate ceramics, have been developed for multiple clinical situations owing to their osteoconduction [5,6]. Hydroxyapatite (HA) is a typical bioactive calcium phosphate material for bone grafting [7,8]. Although HA has excellent biocompatibility, it also exhibits poor absorption properties, which increases the risk of secondary infection [9]. β-Tricalcium phosphate (β-TCP) is a representative bioactive calcium phosphate material. β-TCP spontaneously dissolves via hydrolytic degradation under physiological conditions [10,11]. The absorption rate of β-TCP is higher than that of natural bone minerals, indicating that the rate of β-TCP absorption does not correspond to that of bone formation [12].

It is well known that some parts of natural bone tissue in humans are constituted by carbonate apatite (CO_3Ap), which is replaced both the hydroxyl and phosphate sites of HA with carbonate ions [13]. The absorption properties of CO_3Ap are affected by the content ratio of carbonate ion which reduce crystallinity within the apatite structure, thereby enhancing bone reformation or turnover. Importantly, CO_3Ap is absorbed only by osteoclastic absorption; therefore, its absorption rate closely matches that of natural bone [10,14,15]. In addition, the osteoconductivity of CO_3Ap is much higher than that of HA and β-TCP [10]. In the previous clinical study, the safety and efficacy of CO_3Ap for sinus lift procedure were revealed [16]. Some paper reported efficacy of CO_3Ap in the periodontal regeneration of three-wall intrabony defect, or in combination with recombinant human fibroblast growth factor-2 [17,18]. However, as far as author's knowledge, there is no studies applying CO_3Ap alone in one-wall defect for the periodontal regeneration, or analyzing for mineralized dynamics by the bone histomorphometric analysis. Therefore, this study aimed to histologically compare periodontal regeneration of one-wall intrabony defects treated with open flap debridement, β-TCP, and CO_3Ap in dogs.

2. Methods

2.1. Experimental animals

Four healthy 12-month-old male beagle dogs, weighing 10.0–10.9 kg, were used in this study. All dogs were fed a standard soft pellet diet and were allowed to drink water freely during the experiment. The study protocol was approved by the Institutional Animal Care and Use Committee of Tokyo Medical and Dental University (approval number A2020-115C).

2.2. Surgical procedure

First, medetomidine hydrochloride (0.05 mL/kg, Domitor®; Orion Corporation, Espoo, Finland) was administered intramuscularly as premedication. General anesthesia was induced by intravenous injection of sodium thiopental (0.005 mL/kg, Ravonal®; Nipro ES Pharma CO., LTD., Osaka, Japan) under spontaneous breathing. Lidocaine hydrochloride (2% with 1:80000 epinephrine, xylocaine®; GC SHOWAYAKUHIN CORPORATION, Tokyo, Japan) was administered as the local anesthetic. Bilateral mandibular third premolars were extracted, and the socket was allowed to heal for 12 weeks. In the second phase, the animals were anesthetized as in the first phase. One periodontist (S.F.), with extensive experience in regenerative periodontal surgery, performed all procedures in this experiment. A mucoperiosteal flap was elevated (Fig. 1 a,b), and experimental one-wall intrabony defects of 4 × 5 mm were surgically created on distal side of the mandibular bilateral second premolar and mesial side of the fourth premolar (Fig. 1 c,d). Subsequently, the roots were carefully scaled to remove the root cementum and periodontal ligament, using Gracey curettes (Hu-Friedy Co., Chicago, IL, USA). After root planing, a reference notch was created at the apical end of the root surface using a round bur.

Each defect was randomly allocated to one of the following treatment groups: open flap debridement (control), β-TCP granules (OSferion® 150–500 μm granules; Olympus Terumo Biomaterials Corp., Tokyo, Japan), or CO_3Ap granules (Cytrans® 300–600 μm granules; GC Corporation, Tokyo, Japan) (Fig. 1e); each of bone graft materials was loaded to the level of an alveolar crest under moderate pressure. The flap was then closed to its original position with single interruptted sutures (Gore-Tex CV-6 suture; W. L. Gore & Associates, Inc., Newark, DE, USA) (Fig. 1f). After the surgical procedures, an antibiotic (Penicillin G®; Meiji Seika Pharma Co., Ltd., Tokyo, Japan) and analgesic agent (Vetorphale®; Meiji Seika Pharma Co., Ltd.) were administered intramuscularly. Postoperatively, disinfection was performed three times each week for 4 weeks using 2% chlorhexidine solution (Hibitane® concentrate; Sumitomo Seiyaku Co., Ltd.,

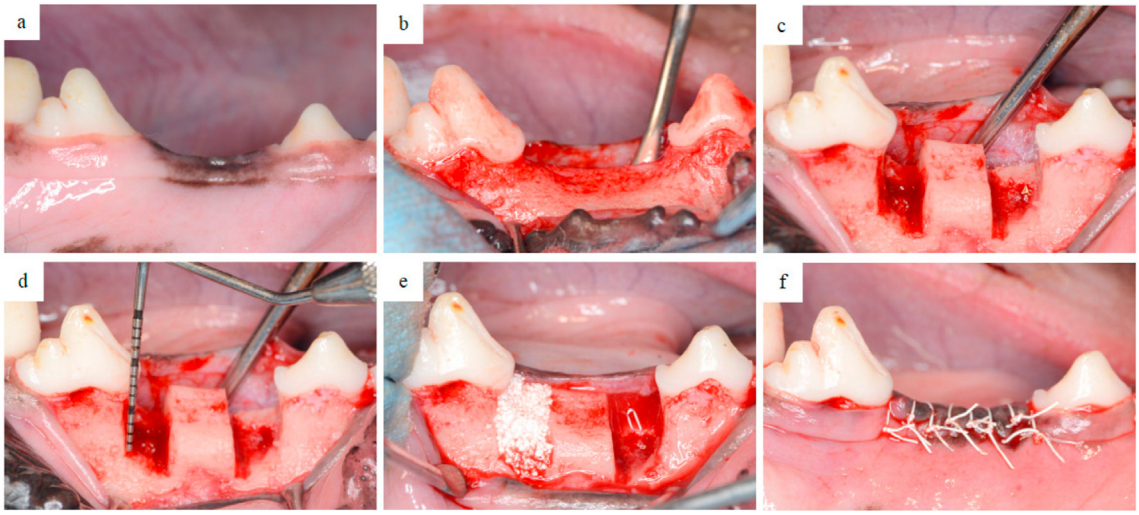

Fig. 1. The surgical procedure used in this study. (a) Before surgical procedure (b) A muco-periosteal flap was elevated. (c) A surgically created bone defect at the first premolar of the mandibular bilateral second premolar distal side and fourth premolar mesial side. (d) Bone defects were trimmed to 4 × 5 mm. (e) Grafted CO_3Ap at the bone defects in the experimental sites. (f) The flap was closed to its original position with single interruptted sutures.

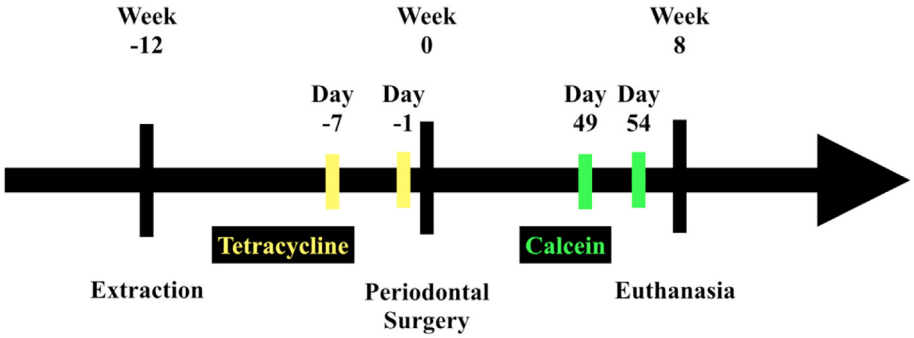

Fig. 2. Overview of the treatment and bone-labeling time course. Tetracycline was injected 1 and 7 days before the surgical procedure. Calcein was similarly administered 2 and 7 days before euthanasia.

Osaka, Japan) for oral rinse. After 2 weeks of healing, the sutures were removed. Eight weeks postoperatively, all dogs were euthanized via overdose of sodium thiopental.

2.3. Image analysis: micro-computed tomography

A micro-computed tomography system (inspeXio SMX-100CT; Shimadzu Co., Kyoto, Japan) was used to capture the images at a voltage of 75 kV and current of 30 μA. The scanned data were reconstructed into two and three-dimensional images using an image analysis software (TRI/3D-BON; Ratoc System Engineering Co., Ltd., Tokyo, Japan).

2.4. Histological analysis

The time-course of the bone labeling was summarized in Fig. 2. Tetracycline (Tetracycline®; Sigma-Aldrich, St. Louis, MO, USA) was injected subcutaneously at 20 mg/kg (per kg body weight), and bone labeling was performed 1 and 7 days before the surgical procedure. Bone labeling with calcein (CL®; Sigma-Aldrich) was similarly administered at 20 mg/kg (per kg body weight), subcutaneously injected 2 and 7 days before euthanasia. The samples were fixed in 70% ethanol and stained with Villanueva Bone Stain. Then, the samples were embedded in methyl methacrylate in a undecalcified state. Polished sections were prepared at the center of the defect, as confirmed by micro-computed tomography imaging. The sections were observed under an optical microscope (bz-x700; Keyence, Osaka, Japan). Measurements wereperfoemed using image processing software (ImageJ v.1.43u; National Institutes of Health). The following parameters were measured.

(1) Defect width: the distance from the root of the tooth to the boundary between the new and existing bone.
(2) Defect depth: length at a 4 to 5 ratio of the defect width.
(3) Alveolar bone height: the distance between the apical extent of the root planing and the coronal extent of the newly formed alveolar bone along the root surface.
(4) Ratio of alveolar bone height: alveolar bone height/defect height.
(5) New cementum length: the distance between the apical extent of the root planing and the coronal extent of the newly formed cementum on the denuded root surface.
(6) Ratio of new cementum length: new cementum length/defect height.
(7) Defect area: the area of a parallelogram whose width is the width of the defect.
(8) Ratio of new bone area: percentage of bone tissue in the defect area.
(9) Ratio of residual granules: the percentage area occupied by residual granules in the defect area.
(10) Bone contact percentage: the percentage of surface of the residual granules directly contacting to new bone.

The parameters were measured by a single experienced blinded examiner (M.O.).

2.5. Bone histomorphometric analysis

The sections were observed using the same optical microscope under the fluorescent light. The measured parameters were as follows.

(11) Inter-label thickness: width of the calcein-labeled green line at the alveolar bone crest.
(12) Mineral apposition rate (MAR): inter-label thickness/day.

2.6. Statistical analyses

The mean and standard deviation for each parameter were calculated for each treatment group using the values obtained from the animals ($n = 4$). Tukey's test and Wilcoxon rank-sum test were used to analyze differences between groups. Statistical significance was set at $p < 0.05$. All statistical analyses were performed using EZR (Saitama Medical Center, Jichi Medical University, Saitama, Japan), a graphical user interface for R (The R Foundation for Statistical Computing, Vienna, Austria); it is a modified version of the R commander designed to add statistical functions frequently used in biostatistics [19].

3. Results

3.1. Clinical observation

After the surgical procedure, healing progressed without clinical problems at any site, and no inflammatory findings were observed. No exposed bone graft substitutes, increased tooth mobility, infection, or suppuration was observed during the observation period.

3.2. Micro-computed tomography observations

Three-dimensional images of micro-computed tomography showed increasing radiopacity in the surgically created defect area in all experimental groups (Fig. 3 a–f). The boundary between the original bone and the experimental area was indistinct in all

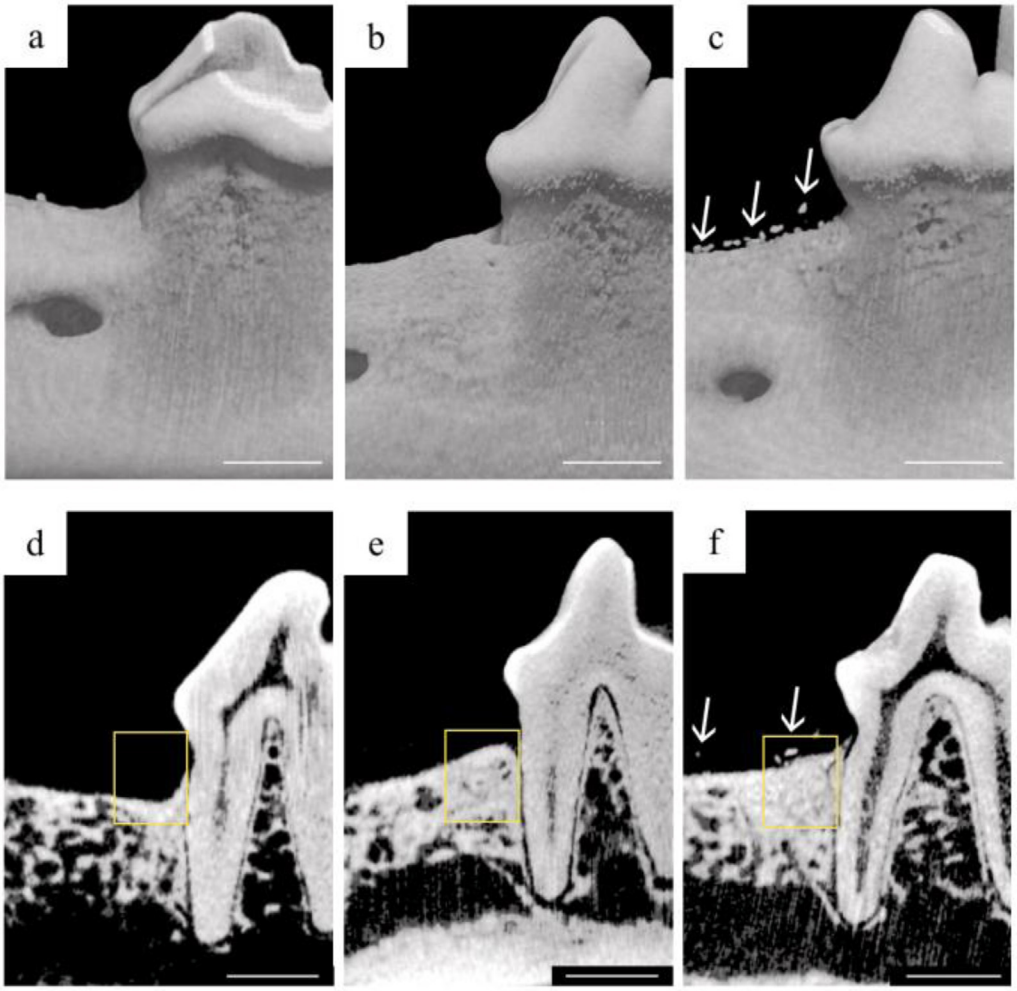

Fig. 3. Micro-computed tomography evaluation. 3D (a–c) and 2D (d–f) micro-computed tomography mesio-distal images revealed bone-like radiopacity within the defects at all sites. Images were obtained from the (a, d) control, (b, e) β-TCP, and (c, f) CO_3Ap groups. Images within the yellow framed area are regions of interest. Scale bars = 5 mm. Residual CO_3Ap granules (white arrows).

groups, and the alveolar bone was continuous. In the β-TCP and CO_3Ap groups, the created bone defects were almost entirely filled with bone-like tissue, including residual granules. At the control site, alveolar bone regeneration was observed, but the defect was not completely filled with hard tissue and was concaved at the distal side of the root.

3.3. Histologic observations

Inflammatory cell infiltration and ankylosis were not observed at any of the experimental sites (Fig. 4 a–c).

In the control group, new bone was formed along the root plane and the crest reached the middle of the planed root surface. This new bone surface was concave in the defect area (Fig. 4a). On the other hand, newly formed bone was observed less concave on the surface in the β-TCP group and the CO_3Ap group (Fig. 4 b,c).

In the β-TCP group, various size of residual granules were observed at all sites. Although a few residual granules were observed in the newly formed bone, almost all residual granules were observed in the keratinized gingiva (Fig. 4 b,g). Residual granules were also observed at all sites in the CO_3Ap group. The number of CO_3Ap granules was greater than that in the β-TCP group. New bone formation was observed directly on the surface of the granules without any fibrous tissue. Most CO_3Ap granules were entirely buried with new bone; notably, this was not observed in the β-TCP group (Fig. 4 c,h). Most residual CO_3Ap granules were observed in the newly formed bone, and some granules were observed in the keratinized gingiva. Osteoid tissues were formed on the surface of the new bone. Osteoblasts were observed in a line. Some surfaces of the residual granules were resolved, and osteoclast-like cells were observed (Fig. 4i).

New cementum was observed in all groups, except in the alveolar bone crest of one control sample. Thick new cementum was observed in the CO_3Ap group.

New periodontal ligament were observed at all groups. However, the density of the fibers was low in the control group and almost all the fibers were attached to the new bone (Fig. 5a). The periodontal ligament were inserted only into the new bone, not into the cementum, at two sites in the β-TCP group (Fig. 5b). Various degrees of collagen fiber density were observed. In the CO_3Ap group, new periodontal ligaments were inserted into the new bone and the new cementum (Fig. 5c). Dense fiber was observed, although the density varied.

3.4. Histological analysis

The results of the histomorphometric measurements are summarized in Table 1. There were no significant differences among the

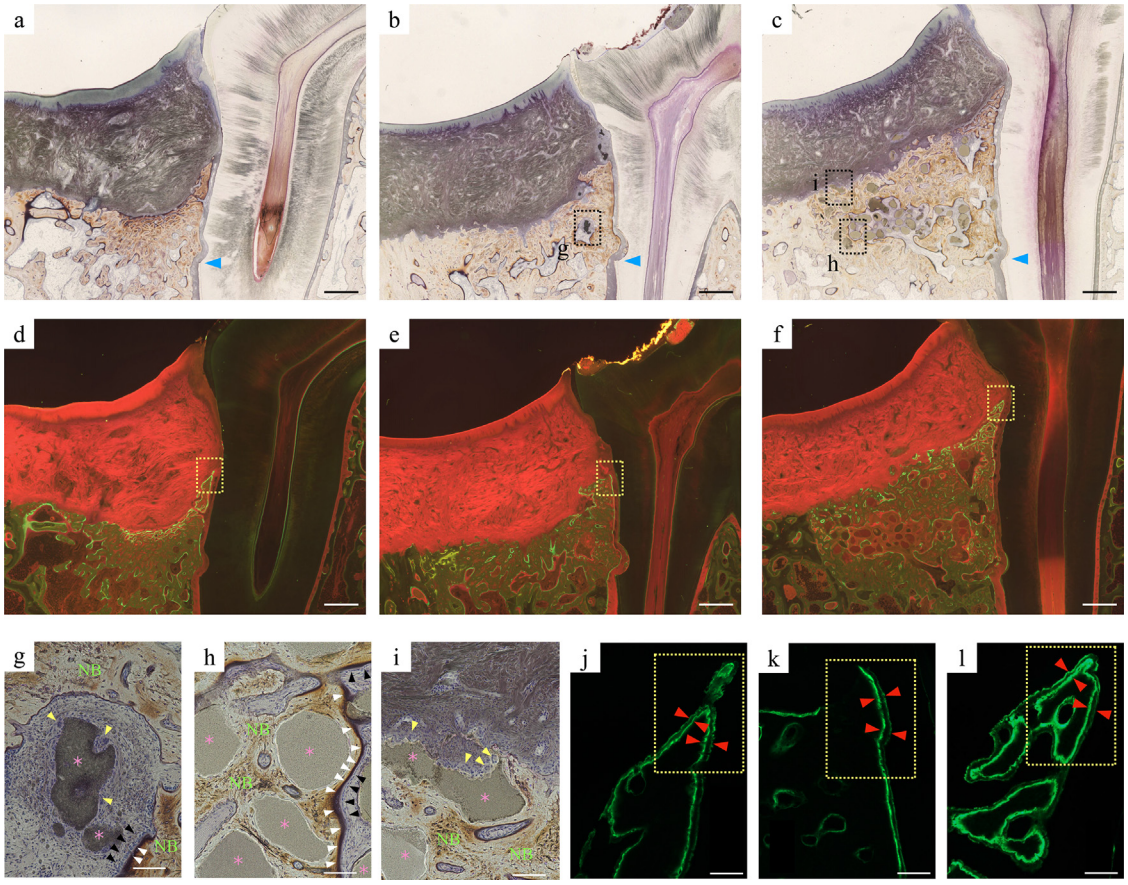

Fig. 4. Villanueva bone staining overview under natural light (a–c) and fluorescence (d–f) microscopy. Histological observations of the bone defects in the (a, d) control, (b, e) β-TCP, and (c, f) CO_3Ap groups. There was no evidence of infection or acute inflammation in all experimental sites. Higher magnification images (g–i) were obtained from (b, c). (g) β-TCP granules still remained, and new bone formation, and osteoblast cells were not observed around the β-TCP granules directly. Osteoclast-like giant cells (yellow arrowheads) were observed around the β-TCP granules. (h, i) CO_3Ap granules still remained. Some CO_3Ap granules were entirely submerged in newly formed bone. Osteoid tissues (white arrowheads) were formed on the surface of the new bone. Osteoblasts (black arrowheads) were observed in a line. Osteoclast-like giant cells (yellow arrowheads) were observed on the surface of some CO_3Ap granules (i). Higher magnification images (j–l) were obtained from the framed area in (d–f). Inter-label thickness stained by calcein green was measured as the width between red arrowheads. No fluorescent tetracycline bone labeling was observed in the defect area in all groups. blue arrowheads; notch. NB; new bone. *; residual granules. (a–f) Scale bars = 1 mm. (g–l) Scale bars = 100 μm.

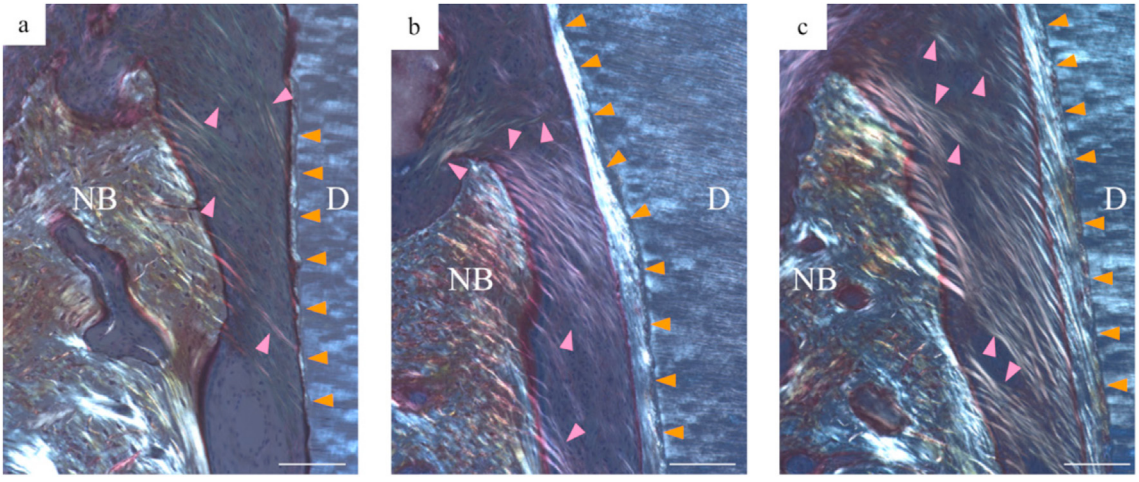

Fig. 5. Representative photomicrographs at the alveolar bone crest through the polarized light. Newly formed periodontal ligament for sites receiving (a) control, (b) β-TCP, and (c) CO_3Ap groups. D, dentin; NB, new bone; orange arrowheads, new cementum; pink arrowheads, new periodontal ligaments; scale bars = 100 μm.

Table 1
Histomorphometric measurements.

Parameter	Control	β-TCP	CO_3Ap	Statistically significant differences
Ratio of alveolar bone height (%)	31.9 ± 12.5	59.2 ± 18.7	65.3 ± 13.3	NS
Ratio of new cementum (%)	20.0 ± 10.9	23.1 ± 14.1	33.3 ± 10.7	NS
Ratio of new bone area (%)	37.7 ± 11.7	62.1 ± 12.3	76.9 ± 21.4	1 versus 3*

Note: Tukey's test was used. Results are given as mean ± standard deviation.
*$P < 0.05$ (significant difference); n = 4.

treatment groups in the ratio of alveolar bone height (ABH) and the ratio of new cementum length. However, the β-TCP and CO_3Ap groups showed higher values than the control group. There was a significant difference between the CO_3Ap and control groups regarding the percentage of the new bone area (NBA) ($P < 0.05$). Between the β-TCP and control groups, the percentage of NBA was not reached to the significantly different.

The results of the histological analysis of residual granules measurements are summarized in Table 2. There were no significant differences between the β-TCP and CO_3Ap groups regarding the ratio of the residual granules area. However, the CO_3Ap group showed higher values than the β-TCP group. There was a significant difference between the CO_3Ap and β-TCP groups regarding the bone contact percentage ($P < 0.05$).

3.5. Bone histomorphometric analysis

The results of the bone histomorphometric analysis are summarized in Table 3. Bone histomorphometric measurements revealed the MAR values were 3.14 ± 0.46 μm/day, 4.82 ± 1.11 μm/day, and 5.13 ± 1.23 μm/day in the control, β-TCP, and CO_3Ap groups, respectively (Fig. 4 j–l). There was no significant difference in the MAR of the alveolar crest between the β-TCP and CO_3Ap groups. However, the β-TCP and CO_3Ap groups showed higher values than the control group. No fluorescent tetracycline bone labeling was observed in all groups.

4. Discussion

This preclinical study showed that CO_3Ap was safe and effective bone graft substitutes for periodontal regeneration in one-wall intrabony defect. Histomorphometric analysis revealed that the ratio of the new bone area was significantly higher in the CO_3Ap group than in the control group. Additionally, the bone contact percentage of the residual granules was significantly higher in the CO_3Ap group than in the β-TCP group. The favorable outcomes in terms of MAR were observed in the CO_3Ap and β-TCP groups compared to the control group. These findings indicate that the CO_3Ap has great potential in periodontal regeneration and might have superior osteoconductivity compare to the β-TCP.

In this study, periodontal tissue regeneration was observed in all groups, and no inflammatory or infectious findings were observed. Although encupsled residual granules were observed in keratinized gingiva, there was no inflammatory cell infiltration around the granules, suggesting that the material has excellent biocompatibility *in vivo*.

Table 2
Histological analysis of residual granule measurements.

Parameter	β-TCP	CO_3Ap
Ratio of residual granules (%)	2.4 ± 4.7	12.2 ± 10.3
Bone contact percentage (%)	10.5 ± 9.5	62.5 ± 21.3*

Note: Wilcoxon rank-sum test was used. Results are given as mean ± standard deviation.
*$P < 0.05$ (significant difference); n = 4.

The CO_3Ap and β-TCP groups showed greater percentages of ABH and NBA than the control group. There were no significant differences in the percentage of ABH among the experimental groups in terms of the ABH ratio. However, there were significant differences between the CO_3Ap and control groups in the ratio of NBA. These findings are supported by the previous studies demonstrating that bone grafts may maintain sufficient space and blood clot stability, and prevent flap collapse in non-contained defects [2,20,21].

It has been reported that the enhanced osteogenic ability of CO_3Ap is caused by the release of calcium ions, which can bind to the cell membrane via G protein-coupled receptors to activate the extracellular signal-related kinase pathway [22,23]. Furthermore, a much higher osteoconductivity of CO_3Ap was reported compared to that of β-TCP [10]. These reports are consistent with our study. In the point of view, there was a significant difference in the bone contact percentage between the CO_3Ap and control groups. There were also significant differences in the NBA percentage between the CO_3Ap and control groups, but not between the β-TCP and control groups.

In the present study, the ratio of new cementum was higher in the CO_3Ap group than in the β-TCP group. However, no significant differences were observed between the groups. This may be because calcium ions promote cementogenesis and recruit STRO-1-positive mesenchymal periodontal ligament cells to undergo cementoblast differentiation and mineralization [24].

Regarding with the ratio of residual granules, it was higher in the CO_3Ap group than in the β-TCP group, although no significant differences were observed. β-TCP has higher solubility in physiological saline [25]. CO_3Ap is stable in physiological saline, and is absorbed only by osteoclasts; therefore, its absorption rate is slower than that of β-TCP [10,14,15]. This may be due to the smaller size of β-TCP granules and their absorption rate *in vivo* [26,27]. Indeed, osteoclast-like giant cells were observed around the both particles of β-TCP and CO_3Ap (Fig. 4 g,i).

In this study, there were no significant differences in the ABH, new cementum, and the ratio of residual granules. However, there were tendencies toward higher ratios in the CO_3Ap group than in the others. The results were based on a small number of experimental animals (four beagle dogs). Further standardized studies, including a larger number of experimental animals, are needed to clarify the characteristics of CO_3Ap.

Regarding bone formation, there are some previous studies reported that CO_3Ap for guided bone regeneration revealed favorable bone formation [28]. One of these studies, CO_3Ap might affect not only bone formation but also new cementum and new periodontal ligament formation. Previous studies have reported that in periodontal tissues, owing to carbonate and calcium ion effects, the use of CO_3Ap resulted in enhanced promotion of osteoclast migration and osteoblast differentiation and more significant bone formation compared to deproteinized bovine bone mineral (DBBM) and β-TCP in canine three-wall intrabony defects [28,29]. These promising results are broadly consistent with the present findings showing

Table 3
Bone histomorphometric analysis.

Parameter	Control	β-TCP	CO_3Ap	Statistically significant differences
MAR (μm/day)	3.14 ± 0.46	4.82 ± 1.11	5.13 ± 1.23	NS

Note: Tukey's test was used. Results are given as mean ± standard deviation. n = 4.

mature osteogenesis and osteoclast recruitment around residual CO_3Ap granules that exhibit higher osteoconductivity than β-TCP [18].

In an attempt to better understand histomorphometric findings, tetracycline and calcein were used as a fluorescent reagent to measure bone formation activity in this study. It is well known that tetracycline and calcein are labeled and appeared under fluorescence microscopy as yellow and green line, respectively. Quantitative assessment of bone formation using double labellings between different time points were performed. In other words, the width between the labels corresponded to the thickness of the formed bone during this period. In this study, fluorescent tetracycline bone labellings were not observed in the defect area in all groups. The labellings could be observed in the area of the original bone, however, most of them were not clear enough to calculate the width between them. It indicated that bone metabolism might be normally quite low in large animals such a beagle dog. Additionally, this finding might be also derived from the different bone formation activity between the alveolar bone and other bony parts of the body.

In contrast, calcein bone labellings were cleary observed in all groups. Bone formation activity was apparently promoted by the periodontal surgery. The CO_3Ap and β-TCP groups showed greater MAR values than the control group, although there were no statistically significant differences. This finding might indicate that bone grafting leads to bone regeneration in the entire defect. This may be because periodontal tissue regeneration is reinforced by bone graft materials. This is supported by previous reports that bone graft material stabilized a space for tissue regeneration, blood clots, and the flap position in non-contained defects [2,20,21].

In the previous reports, Sato [17] and Shirakata [18] compared the regenerative ability of CO_3Ap to that of DBBM. DBBM is composed of low-absorbable demineralized bovine bone and is recommended for its biocompatibility and new bone formation properties [30]. DBBM is known for its slower degradation rate; it requires more time for bone replacement compared with β-TCP and CO_3Ap. In the present study, we did not directly compare CO_3Ap with DBBM. It is necessary to conduct further studies comparing these in the future.

We must consider that the present study was conducted in young, healthy beagle dogs, which heal faster than humans, and in an acute model in which periodontal defects were created surgically, rather than in a chronic model, under conditions in which healing was likely to occur [31,32].

In this study, we conducted only bone grafting, without using a growth factor or a barrier membrane, to evaluate the ability of the graft materials. However, bone graft materials are rarely used alone for periodontal tissue regeneration therapy for one-wall intrabony defects; they are commonly used with growth factors and membranes [33]. DBBM has been reported to be more effective than CO_3Ap or β-TCP when used in combination with recombinant human fibroblast growth factor-2 [18]. Reports on CO_3Ap in combination with recombinant human fibroblast growth factor-2 are still limited, and combinations with other materials have not been reported. Therefore, further studies are warranted. Other standardized experimental and human studies are required to determine whether the results of this study are consistent with clinical findings in patients with periodontal disease.

5. Conclusion

Although this study has limitations, the findings revealed the safety and efficacy of CO_3Ap for periodontal regeneration in one-wall intrabony defects in dogs, and CO_3Ap might have a better ability to integrate with bone than β-TCP.

Author contributions

S.F., M.O., T.M., S.H., and T.I. conceived the study design. S.T., S.F., M.O., K.N., R.S., D.Y., T.M., and S.H. did the animal experiment. S.T., S.F., and M.O. performed data acquisition and analysis. K.A. supervised bone histomorphometric analysis. S.T. drafted the manuscript. S.T., S.F., M.O., R.S., T.M., S.H., K.A., and T.I. revised the manuscript. All authors have read and approved the final manuscript.

Declaration of competing interest

This study received funding from GC Corporation (Tokyo, Japan). The funder had the following involvement with the study design, interpretation of data. The remaining authors declare that the research was conducted in the absence of any commercial or financial relationships that could be construed as a potential conflict of interest.

Acknowledgments

We are grateful to Ayako Mimata (Research Core, Tokyo Medical and Dental University, Tokyo, Japan) for her advice and support in processing histological analysis.

References

[1] Papapanou PN, Tonetti MS. Diagnosis and epidemiology of periodontal osseous lesions. Periodontol 2000 2000;22:8–21.
[2] Cortellini P, Tonetti MS. Clinical concepts for regenerative therapy in intrabony defects. Periodontol 2000 2015;68:282–307.
[3] Brunsvold MA, Mellonig JT. Bone grafts and periodontal regeneration. Periodontol 2000 1993;1:80–91.
[4] Sheikh Z, Hamdan N, Ikeda Y, Grynpas M, Ganss B, Glogauer M. Natural graft tissues and synthetic biomaterials for periodontal and alveolar bone reconstructive applications: a review. Biomater Res 2017;21:9.
[5] Bouler JM, Pilet P, Gauthier O, Verron E. Biphasic calcium phosphate ceramics for bone reconstruction: a review of biological response. Acta Biomater 2017;53:1–12.
[6] Endres M, Hutmacher DW, Salgado AJ, Kaps C, Ringe J, Reis RL, et al. Osteogenic induction of human bone marrow-derived mesenchymal progenitor cells in novel synthetic polymer-hydrogel matrices. Tissue Eng 2003;9:689–702.
[7] Donath K, Rohrer MD, Beck-Mannagetta J. A histologic evaluation of a mandibular cross section one year after augmentation with hydroxyapatite particles. Oral Surg Oral Med Oral Pathol 1987;63:651–5.
[8] Bauer TW, Muschler GF. Bone graft materials. An overview of the basic science. Clin Orthop Relat Res 2000:10–27.
[9] Moore WR, Graves SE, Bain GI. Synthetic bone graft substitutes. ANZ J Surg 2001;71:354–61.
[10] Doi Y, Iwanaga H, Shibutani T, Moriwaki Y, Iwayama Y. Osteoclastic responses to various calcium phosphates in cell cultures. J Biomed Mater Res 1999;47:424–33.
[11] Yamasaki N, Hirao M, Nanno K, Sugiyasu K, Tamai N, Hashimoto N, et al. A comparative assessment of synthetic ceramic bone substitutes with different composition and microstructure in rabbit femoral condyle model. J Biomed Mater Res B Appl Biomater 2009;91:788–98.
[12] Kwon SH, Jun YK, Hong SH, Lee IS, Kim HE, Won YY. Calcium phosphate bioceramics with various porosities and dissolution rates. J Am Ceram Soc 2002;85:3129–31.

[13] Rey C, Collins B, Goehl T, Dickson IR, Glimcher MJ. The carbonate environment in bone mineral: a resolution-enhanced Fourier Transform Infrared Spectroscopy Study. Calcif Tissue Int 1989;45:157–64.
[14] Hasegawa M, Doi Y, Uchida A. Cell-mediated bioresorption of sintered carbonate apatite in rabbits. J Bone Joint Surg Br 2003;85:142–7.
[15] Doi Y, Shibutani T, Moriwaki Y, Kajimoto T, Iwayama Y. Sintered carbonate apatites as bioresorbable bone substitutes. J Biomed Mater Res 1998;39:603–10.
[16] Nakagawa T, Kudoh K, Fukuda N, Kasugai S, Tachikawa N, Koyano K, et al. Application of low-crystalline carbonate apatite granules in 2-stage sinus floor augmentation: a prospective clinical trial and histomorphometric evaluation. J Periodontal Implant Sci 2019;49:382–96.
[17] Sato N, Handa K, Venkataiah VS, Hasegawa T, Njuguna MM, Yahata Y, et al. Comparison of the vertical bone defect healing abilities of carbonate apatite, beta-tricalcium phosphate, hydroxyapatite and bovine-derived heterogeneous bone. Dent Mater J 2020;39:309–18.
[18] Shirakata Y, Setoguchi F, Sena K, Nakamura T, Imafuji T, Shinohara Y, et al. Comparison of periodontal wound healing/regeneration by recombinant human fibroblast growth factor-2 combined with beta-tricalcium phosphate, carbonate apatite, or deproteinized bovine bone mineral in a canine one-wall intra-bony defect model. J Clin Periodontol 2022;49:599–608.
[19] Kanda Y. Investigation of the freely available easy-to-use software 'EZR' for medical statistics. Bone Marrow Transplant 2013;48:452–8.
[20] Lekovic V, Camargo PM, Weinlaender M, Nedic M, Aleksic Z, Kenney EB. A comparison between enamel matrix proteins used alone or in combination with bovine porous bone mineral in the treatment of intrabony periodontal defects in humans. J Periodontol 2000;71:1110–6.
[21] Polimeni G, Koo KT, Qahash M, Xiropaidis AV, Albandar JM, Wikesjö UM. Prognostic factors for alveolar regeneration: effect of a space-providing biomaterial on guided tissue regeneration. J Clin Periodontol 2004;31:725–9.
[22] Seol YJ, Park JY, Jung JW, Jang J, Girdhari R, Kim SW, et al. Improvement of bone regeneration capability of ceramic scaffolds by accelerated release of their calcium ions. Tissue Eng 2014;20:2840–9.
[23] Hofer AM, Lefkimmiatis K. Extracellular calcium and cAMP: second messengers as "third messengers". Physiology 2007;22:320–7.
[24] Paula-Silva FW, Ghosh A, Arzate H, Kapila S, da Silva LA, Kapila YL. Calcium hydroxide promotes cementogenesis and induces cementoblastic differentiation of mesenchymal periodontal ligament cells in a CEMP1- and ERK-dependent manner. Calcif Tissue Int 2010;87:144–57.
[25] Fujita R, Yokoyama A, Kawasaki T, Kohgo T. Bone augmentation osteogenesis using hydroxyapatite and beta-tricalcium phosphate blocks. J Oral Maxillofac Surg 2003;61:1045–53.
[26] Ridgway HK, Mellonig JT, Cochran DL. Human histologic and clinical evaluation of recombinant human platelet-derived growth factor and beta-tricalcium phosphate for the treatment of periodontal intraosseous defects. Int J Periodontics Restor Dent 2008;28:171–9.
[27] Shirakata Y, Takeuchi N, Yoshimoto T, Taniyama K, Noguchi K. Effects of enamel matrix derivative and basic fibroblast growth factor with μ-tricalcium phosphate on periodontal regeneration in one-wall intrabony defects: an experimental study in dogs. Int J Periodontics Restor Dent 2013;33:641–9.
[28] Mano T, Akita K, Fukuda N, Kamada K, Kurio N, Ishikawa K, et al. Histological comparison of three apatitic bone substitutes with different carbonate contents in alveolar bone defects in a beagle mandible with simultaneous implant installation. J Biomed Mater Res B Appl Biomater 2020;108:1450–9.
[29] Lee MN, Hwang HS, Oh SH, Roshanzadeh A, Kim JW, Song JH, et al. Elevated extracellular calcium ions promote proliferation and migration of mesenchymal stem cells via increasing osteopontin expression. Exp Mol Med 2018;50:1–16.
[30] Orsini G, Traini T, Scarano A, Degidi M, Perrotti V, Piccirilli M, et al. Maxillary sinus augmentation with Bio-Oss particles: a light, scanning, and transmission electron microscopy study in man. J Biomed Mater Res B Appl Biomater 2005;74:448–57.
[31] Wikesjö UM, Selvig KA, Zimmerman G, Nilvéus R. Periodontal repair in dogs: healing in experimentally created chronic periodontal defects. J Periodontol 1991;62:258–63.
[32] Pellegrini G, Seol YJ, Gruber R, Giannobile WV. Pre-clinical models for oral and periodontal reconstructive therapies. J Dent Res 2009;88:1065–76.
[33] Kao RT, Nares S, Reynolds MA. Periodontal regeneration - intrabony defects: a systematic review from the AAP Regeneration Workshop. J Periodontol 2015;86:S77–104.